Disruption without diversity loss: how spreading thermotolerant *Pilidium lythri* infection perturbs plant-soil microbiome stability

Dominika Siegieda[1*]

Jacek Panek[1]

S. Emilia Hannula[2]

Magdalena Frąc[1]

[1]Institute of Agrophysics, Polish Academy of Sciences, Doświadczalna 4 street, 20-290 Lublin, Poland

[2]Leiden University, Institute of Environmental Sciences, Department of Environmental Biology, Leiden, The Netherlands

correspondence: Dominika Siegieda (d.siegieda@ipan.lublin.pl)

Keywords

microbiome destabilization, emerging fungal phytopathogen, *Pilidium lythri*, plant holobiont, Anna Karenina Principle, microbial migration, thermotolerance, climate change adaptation

Abstract

While global warming accelerates phytopathogen spread, still little is known on how fungal pathogens disrupt fragile balance in plant-microbe interactions. Here, we demonstrate that the thermotolerant fungus *Pilidium lythri* combines broad chemical resistance with a remarkable ability to destabilize microbial communities in strawberry soil-plant systems. Using high-throughput sequencing (16S rRNA and ITS markers) across 72 samples, combined with mixed-effects modelling,

source-tracking, microbiota assembly mechanisms investigation and network analysis we demonstrate that *P. lythri* disrupted bacterial community assembly processes, transitioning from deterministic to stochastic dynamics in the bulk soil, aligning with the Anna Karenina Principle. Despite stable dominance index (ENS) under infection bacterial and fungal communities, rhizosphere fungal diversity increased under infection. Network analysis of this niche revealed decreased fungal connectivity, with enhanced antagonistic interactions between taxa. We also noted that microbial migration patterns between niches under pathogen inoculation highlighted shifts in community interactions. Our work uncovers how emerging thermotolerant fungal phytopathogens destabilize plant holobiont without reducing diversity, important for managing emerging agricultural threats in a warming climate.

Introduction

Fungal and bacterial microorganisms, together with their host plants, are interconnected through intricate, multi-level interactions that shape ecosystems and sustain plant health and productivity. Based on these relationships, the plant holobiont concept was formed - an integrated system where hosts and microbiota function as one. Plants produce root exudates to modulate microbial assembly of their niches and vicinity, while the microbiome, in turn, is able to influence and regulate plant health, improving its resilience against abiotic and biotic stressors (Berg, 2009; Baldrian, 2016; Trivedi *et al.*, 2020; Gupta *et al.*, 2021; Marco *et al.*, 2022; Michl *et al.*, 2023). These finely tuned interactions are widely studied and hold great potential for improving agricultural productivity in a sustainable manner (Trivedi *et al.*, 2020; Vishwakarma *et al.*, 2020; Frąc *et al.*, 2022).

However, this delicate balance between microbiomes and plants is being increasingly threatened by ongoing global warming. The rise of annual global temperature and changed precipitation patterns has created the opportunity for a spread and establishment of invasive phytopathogens into new regions (Bebber *et al.*, 2013; Helfer, 2014; Liu *et al.*, 2019). Although substantial attention has been given to beneficial plant–microbe interactions, far less is known about how invasive or

47 thermotolerant fungal pathogens perturb microbial community structure, niche interactions and
48 assembly rules. This knowledge gap is particularly concerning for perennial crops like strawberries
49 (*Fragaria x ananassa* Duch.), which depend heavily on stable rhizosphere and soil microbial
50 communities to thrive and are particularly vulnerable to such disruptions.

51 Ecological theory offers a conceptual lens for understanding such perturbations. The *Anna Karenina*
52 *Principle* (AKP) predicts that under biotic or abiotic stress, host-associated microbiomes become
53 more variable and stochastic and unpredictible. Increasing evidence suggests that pathogen-induced
54 disruption can generate divergent microbiome states rather than uniform shifts, but experimental
55 demonstrations in soil–plant systems remain limited (Arnault *et al.*, 2023).

56 *Pilidium lythri* is an emerging fungal phytopathogen with a versatile host range and limited genomic
57 data. This ascomycete was originally reported in countries located in warmer climate zones, such as
58 India (Phatak and Payak, 1965), Iran (Arzanlou *et al.*, 2013; Sayami *et al.*, 2013) and China (Zhang *et*
59 *al.*, 2008; Duan *et al.*, 2010). Notably, its occurrence had been recently identified in several
60 temperate climate countries, including Belgium (Debode *et al.*, 2011), Croatia (Milicević *et al.*, 2014),
61 Spain (Aguín *et al.*, 2018), France (Cardin *et al.*, 2009; Caesar *et al.*, 2012) and Poland, although in
62 2004 only morphologically, but in 2020 we confirmed its presence in symptomatic Polish strawberry
63 fields with molecular methods (Gołębniak and Jarosz, 2004; Malarczyk *et al.*, 2020), and with new
64 isolates collected in present study. Primary targets of this fungal phytopathogen are strawberry
65 plants and fruits (Lopes *et al.*, 2010; Geng *et al.*, 2012; Ayoubi *et al.*, 2016), but it also affects other
66 agriculturally significant plants, including *Olea europaea* L. (Arzanlou *et al.*, 2013), *Cornus mas*
67 (Torbati *et al.*, 2019), *Prunus domestica* (Sayami *et al.*, 2013), *Eucalyptus* spp. (Maússe-Sitoe *et al.*,
68 2016), *Vitis vinifera* (Aguín *et al.*, 2018), and various ornamental flowers (Zhang *et al.*, 2008; Cardin *et*
69 *al.*, 2009; Caesar *et al.*, 2012; Bruckart *et al.*, 2013; Garfinkel and Chastagner, 2019). Notably
70 concerning is that *P. lythri* is not host-specific. Strains isolated from olives were able to cause disease
71 symptoms on strawberry fruits (Karimi *et al.*, 2016), further increasing the severity of the threat

posed by this pathogen as it spreads to new regions. Studies conducted in Brazil, Iran and Belgium showed incidence as high as 70% in high humidity and warm temperatures, highlighting its threat in warming climate (Lopes *et al.*, 2010; Ayoubi *et al.*, 2016; Karimi *et al.*, 2016). Pathogenicity test revealed rapid progression of the disease, with symptoms appearing on up to 100% of fruits within days after inoculation (Debode *et al.*, 2011; Fernández-Ortuño *et al.*, 2014). The pathogen is able to infect both wounded and intact grape berries, further underscoring its high virulence (Aguín *et al.*, 2018). Yet, no study has examined how *P. lythri* or other spreading, thermotolerant phytopathogens influence microbial processes in soil–plant interfaces or whether its effects produce AKP-like disruptions in microbial assembly.

Here, we hypothesised that infection by a thermotolerant fuganal pathogen destabilizes microbial community assembly across soil-plany niches, increasing stochasticity and altering microbial interaction patterns consistent with the Anna Karenina Principle. To test this, we (I) explored chemical astress tolerance of *P. lythri* across temperatures, (II) quantified pathogen-induced changes in bacterial and fungal communities in bulk soil, rhizosphere and roots using high-throughput sequencing, and (III) assessed assembly mechanisms, source-sink dynamics and network stability under infection. This approach contribute to a broader understanding how spreading pathogens influence plant-microbiome systems in the face of environmental change.

Methods

Fungal isolates and molecular identification

Pure fungal isolates were obtained by placing symptomatic strawberry leaves and fruits (surface-sterilized with detergent and 70% ethanol) on PDA medium and incubating them at 24°C in darkness for 7 days. After initial screening, fungi with macroscopic and microscopic characteristics matching the description of *P. lythri* (Palm, 1991; Marin-Felix *et al.*, 2017; Karimi *et al.*, 2019) were identified through amplification and Sanger sequencing of the Internal Transcribed Spacer (ITS) regions of fungal rDNA, with ITS1 and ITS4 primers (White *et al.*, 1990), as previously described (Frąc *et al.*,

2015). The obtained sequences were deposited in GenBank under accession numbers: PQ632564.1, PQ632565.1, PQ632566.1, PQ632567.1. These sequences were then used to construct phylogenetic tree with other sequences available in Genbank database from the *Pilidium* genus. Evolutionary analyses were conducted in MEGA X (Kumar *et al.*, 2018). Initial tree for the heuristic search was obtained automatically by applying Neighbor-Join and BioNJ algorithms to a matrix of pairwise distances estimated using the Tamura-Nei model, and then selecting the topology with superior log likelihood value. The tree was drawn to scale, with branch lengths measured in the number of substitutions per site. This analysis involved 57 nucleotide sequences and there were a total of 372 positions in the final dataset. To fulfil Koch's postulates, a spore suspension of 1.6 x 10^4 spores/mL was prepared, and surface-sterilized strawberry leaves were briefly submerged in the solution. The leaves were then sealed in ziplock bags and incubated at 24°C in darkness for 7 days. Sterile deionized water was used as the untreated control.

Metabolic profile arrays

Each cell of Phenotype Microarray 21-25 BIOLOG plates (Biolog, Hayward, CA, USA) was inoculated with the fungal mycelium as recommended by the manufacturer and described before (Panek *et al.*, 2016). The plates are coated with 4 different concentrations of the chemical substances and precise concentrations of the substances used for microarrays are confidential and protected as proprietary information by the manufacturer, thus, for the purposes of this article, we refer to them as concentration levels 1, 2, 3, and 4 to maintain clarity. For each of 120 tested chemical substances (Supplementary Table 1), we incubated 3 *P. lythri* strains across four concentrations at two temperatures (24 and 30°C), resulting in 72 replicates per substance (3 strains x 3 replicates x 4 concentrations x 2 temperatures). The temperature of 24°C reflects the optimal *in vitro* growth conditions for *P. lythri*, while 30°C was selected to simulate elevated temperature scenarios associated with ongoing climate warming. This design allowed us to assess the thermal plasticity of the fungus' metabolic response under environmental shifts. All plates were incubated for 96 hours in the darkness. Microplate reader (Biolog, Hayward, CA, USA) was used to determine the absorbance

at 490 nm at the beginning of the experiment and every 24 hours which reflects the reduction of tetrazolium dye, portraying a metabolic activity of the analysed microorganism. Higher values indicate robust redox activity and potential tolerance against tested chemical. Obtained data was analysed statistically and visualised in RStudio, using tidyverse (Wickham *et al.*, 2019) and lme4 (Bates *et al.*, 2015) packages. First, values obtained at 0 h for each cell was divided from read values at 96 h to establish growth of metabolic activity, and the data was rescaled from 0 to 1. To establish which factors had an influence on fungal activity, we used generalized linear mixed-effects model (GLLM) with Gamma family, controlling for the plate. And to establish whether the substance inhibit fungus' respiration rates, we controlled for plate, strain, temperature and concentration.

Pot experiment and isolation of microbial DNA

Strawberry plants, obtained from the nursery, were grown in pots containing sieved soil from a certified organic strawberry plantation. After 20 days of initial growth of strawberry plants at 29°C and 70% humidity, half of the pots were inoculated with *P. lythri* G322/23 spores using 10 mL of a $2 \cdot 10^4$ spores mL^{-1} solution per plant. Sterile, deionized water was used as a negative control. Samples were collected from two pots in triplicates (6 samples per niche per time point) for healthy and pathogen-inoculated samples in two timepoints: at the time of inoculation and again after 9 days of incubation. Bulk soil was transferred into sterile 1.5 mL Eppendorf tubes and frozen at -20°C. The rhizosphere was collected as described by Lundberg et al. (Lundberg *et al.*, 2012). Roots, flushed free of rhizosphere soil, were also frozen at -20°C prior to DNA isolation which was conducted with the QIAQUBE instrument (Qiagen, Hilden, Germany) and GeneMATRIX Soil DNA Purification Kit (EURx, Gdańsk, Poland) after homogenization of the samples in the FastPrep-24 instrument (MP Biomedicals) at 4 m s^{-1} for 15 s. DNA isolates were then frozen in -20°C until library construction and sequencing.

Metataxonomic sequencing, bioinformatics and statistical analysis

For the metataxonomic sequencing, microbial ITS2 (Schoch *et al.*, 2012) and 16Sv3 regions (Klindworth *et al.*, 2013) were amplified, indexed and sequenced on Illumina MiSeq instrument (2x300). Raw data was deposited at SRA database under accession numbers: PRJNA1213298 for 16S and PRJNA1213307 for ITS. Raw data was then passed through the custom QIIME2 (Bolyen *et al.*, 2019) pipelines as reported before (Siegieda *et al.*, 2023, 2024). In brief, after primer trimming with Cutadapt (Martin, 2011) and ITSxpress (Rivers *et al.*, 2018), denoising, chimera removal, merging and Amplicon Sequence Variant (ASV) calling were performed. The taxonomy was assigned based on UNITE v9 dynamic release (Nilsson *et al.*, 2019) and Silva 138 (Pruesse *et al.*, 2007) databases. The results were then analysed with R (v. 4.0.3), using libraries: phyloseq (McMurdie and Holmes, 2013), tidyverse (Wickham *et al.*, 2019), microeco (Liu *et al.*, 2021), microbiomeMarker (Cao *et al.*, 2022), NetCoMi (Peschel *et al.*, 2021). First, for ITS data, we only used ASVs identified to Fungi and Stramenopiles; and for 16S - Bacteria and Archaea. Then, ITS data was repeatedly rarefied at 6,000 and 16S at 11,000 reads using mirlyn package (McMurdie and Holmes, 2014; Cameron *et al.*, 2021). We used supervised machine learning model to evaluate the fungal biomarkers of each niche for healthy and infected samples with Supervised Machine Method (SVM), using Total Sum Scaling normalization method in microbiomeMarker R library (Cao *et al.*, 2022). We employed Effective Number of Species (ENS) (Jost, 2006) and Simpson index on ASV level to evaluate the dominance of taxa and diversity in each niche. We then used Linear Mixed-Effect Models while controlling for the plant to compare differences between control and infected samples. For the beta-diversity analysis, we used PCoA ordination method based on the weihghthed UniFrac and Bray method for bacteria and fungi. We also used adonis2 (Oksanen *et al.*, 2007) and permutest to compare centroid localisation and dispersion between infection groups. To estimate the migration of the bacterial and fungal communities from the niches (sources) to other niches (sinks), we employed SourceTracker (Knights *et al.*, 2011). This Bayesian method models the proportion of a microbial community in a given sample (sink) that originates from predefined source environments based on shared microbial

taxa. We also used RCbray (Bray-Curtis dissimilarity based Raup-Crick metric) and βNTI (β Nearest Taxon) to evaluate the ecological processes that dominated the bacterial assemblies (Stegen *et al.*, 2013; Liu *et al.*, 2017), using microeco (Liu *et al.*, 2021) R library. βNTI index measures how the differences in species composition between the two samplings differ from what would be expected by the null model of random assembly. When βNTI fell between |2|, microbial assembly was dominated by stochastic mechanisms, and higher than |2|, by deterministic. We then compared the βNTI indexes between control and pathogen-inoculated samples using Wilcoxon signed-rank test. The phylogenetic tree is essential to perform this analysis, we did this only for bacterial communities, as the ITS region is characterised with the variable length for different taxa. Finally, we constructed microbial networks with 200 most frequent taxa and SPIEC-EASI (Sparse Inverse Covariance Estimation for Ecological Association Inference) method (Kurtz *et al.*, 2015), using glasso (Graphical Least Absolute Shrinkage and Selection Operator) approach within NetCoMi R library (Peschel *et al.*, 2021). The dataset was resampled 30 times and 20 penalty levels with 1e-4 as the smallest ratio, taking the average of symmetric edges. Fast greedy clustering method was used for network visualization.

Results

Fungal isolates

Fungal ITS sequences, obtained from symptomatic strawberry leaves (Figure 1B) showed 100% similarity to those of *P. lythri* already present in the GenBank database and phylogenetic tree revealed clustering of the sequences with other representatives of *P. lythri* and *Pilidium concavum* (former name of the *P. lythri* (Marin-Felix *et al.*, 2017)) (Figure 1A). The strains collected after 7 days in 23°C in the darkness on Potato Dextrose Agar were flat and granulose, cinnamon in colour (Karimi *et al.*, 2016; Marin-Felix *et al.*, 2017) (Figure 1E). The presence of hyaline conidia with smooth walls and slightly pointed tips were confirmed under the microscope (Figure 1F). After the inoculation of the surface-sterilized strawberry leaves with the spore suspension and incubation in 24°C in darkness

for 7 days, 100% of the leaves showed brown necrotic lesions. Leaves submerged in water did not show symptoms of the disease (Figure 1C). Growth of the cinnamon-colour fungal strains were observed after incubation (24°C for 7 days) of infested leaves on the Petri dishes with the PDA medium, fulfilling he Koch's postulate (Figure G).

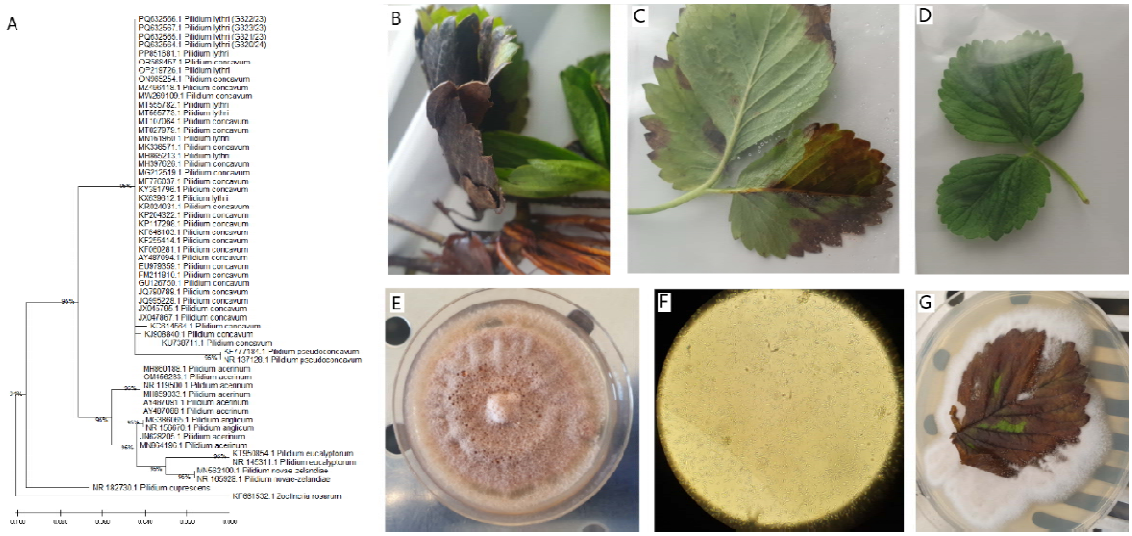

Figure 1. A) Phylogenetic tree of the evolutionary history of *P. lythri* was inferred by using the Maximum Likelihood method and Tamura-Nei model (Tamura & Nei, 1993) and the e tree with the highest log likelihood (-1144.51) is shown. The percentage of trees in which the associated taxa clustered together is shown next to the branches. B,C) Symptoms of the *P. lythri* infection on the strawberry leaves and in the D) control leaf. E) Growth of *P. lythri* after 7 days of growth in 24 °C on PDA medium, F) conidia of *P. lythri* (40x), and G) growth on PDA medium with infected leaf.

Chemical sensitivity

To evaluate *P. lythri*'s sensitivity to various chemicals, BIOLOG PM 21-25 plates were we incubated with the spore and mycelium solution of three fungal strains (G321/23, G322/23, G323/23) at 24°C and 30°C for 96 hours. An evaluation of the GLLM model revealed that, as expected, the temperature increase was positively correlated with fungal metabolic activity growth, and the substance concentration had negative correlation with the fungal metabolic activity. We observed different response of one of strains - G322/23 that was characterised with higher metabolic activity compared to other 2 (Supplementary Figure 1, Supplementary Table 2). We also evaluated substances that negatively impacted metabolic activity (Figure 2). Top inhibitors included thiourea, dodecyltrimethyl

ammonium bromide, tetrazolium violet, alexidine and fluorodeoxyuridine, although the effect size was very small: -0.09, underlining high tolerance of the pathogen to various chemicals.

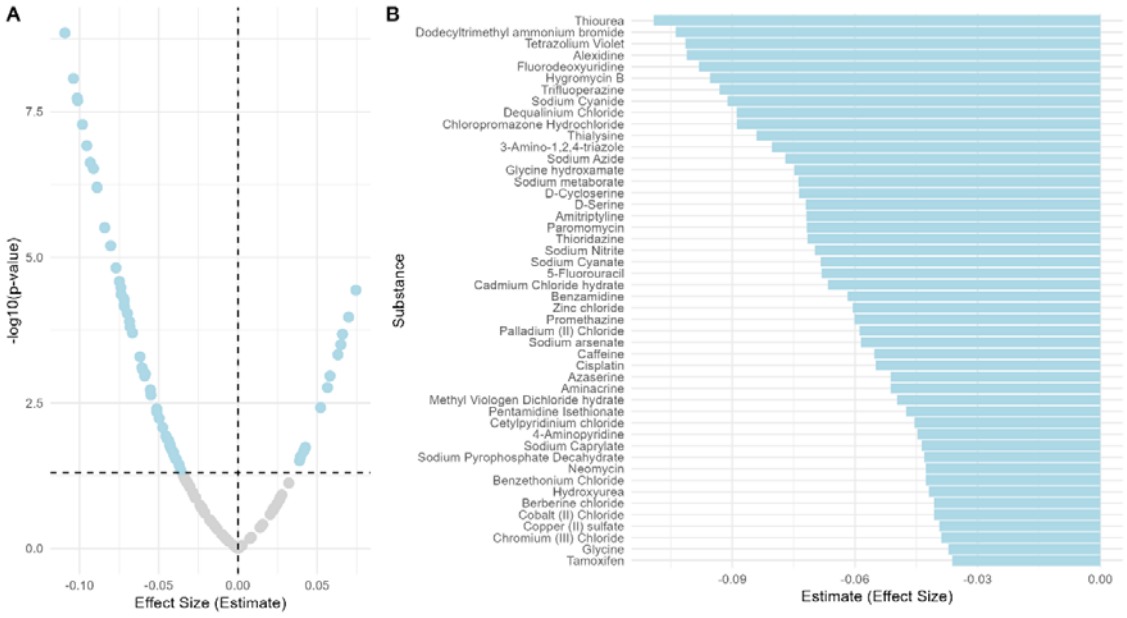

Figure 2. BIOLOG PM21-25 results of the substances that differently influence growth of *P. lythri*. A) Volcano plot visualizing biological and statistical effect for different substances. Gray circles represent no significant importance, light blue - significant results. Dashed vertical lines represent p.value of 0.05 and estimate of -log10(0.05). B) Bar plot representing estimate for each substance significantly inhibiting pathogens metabolic activity in tested conditions.

Fungal and bacterial community changes after *P. lythri* inoculation of strawberry

Fungal and bacterial molecular markers for 72 samples from soil (24), rhizosphere (24), and roots (24) were amplified and sequenced. Rarefaction curves plateaued for all samples, indicating sufficient sequencing depth. To evaluate the presence of *P. lythri* in infected samples, we employed a predictive approach to identify 15 most important bacterial (Supplementary Figure 3) and fungal (Figure 3) taxa that differentiate healthy and infected strawberry compartments. The analysis revealed that the *Pilidium* fungi belonged to the most important taxa that differentiate between healthy and infected plants and soil (Figure 3). This, along with the visible symptoms of the disease,

232 confirmed that the infection was successful and the pathogen migrated from the soil to rhizosphere

233 and roots.

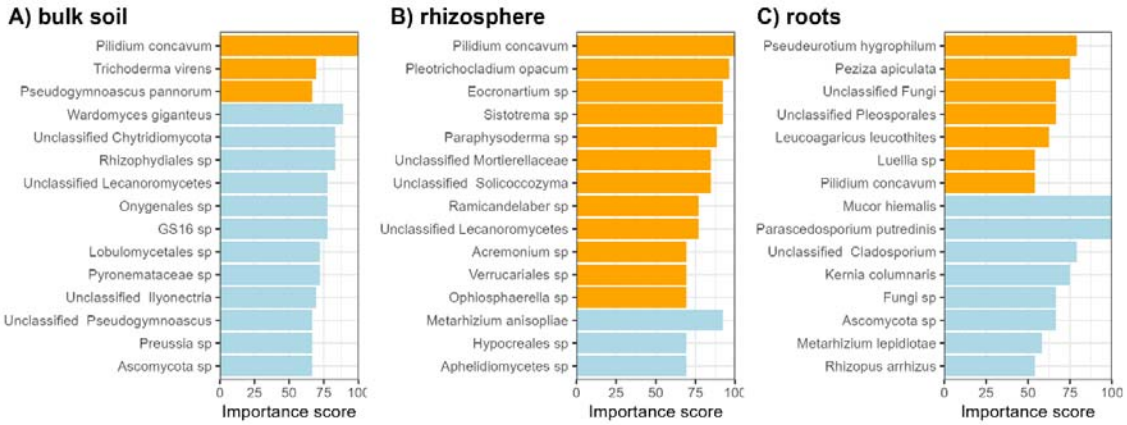

234

235 Figure 3. Top 15 fungal taxa found more abundant in (orange) pathogen-inoculated and in (blue) healthy soils and plants

236 identified based on Supervised Vector Machine machine learning approach.

237 After evaluating that infection was successful, we conducted statistical analysis (LMER modelling

238 while controlling for plant/pot) to compare the alpha diversity of bacterial and fungal communities

239 between healthy and pathogen-inoculated niches. No significant differences in dominance nor

240 richness were observed between healthy and pathogen-inoculated niches at both sampling times (p

241 > 0.05) for bacteria and fungi (Figure 4A, B and Supplementary Table 3). We only noted decreased

242 diversity of fungal microbiome in pathogen-inoculated rhizosphere samples in fungal

243 metacommunities at the second sampling time ($p < 0.05$). We also conducted beta-diversity analysis

244 of the bacterial (Figure 4 C) and fungal (Figure 4 F) communities. We did not see differences between

245 centroid localization for bacteria (PERMANOVA: r^2: 0.019, $p > 0.05$), but the groups were

246 characterized with different dispersions (permutest: $F = 0.0011$, $p < 0.05$), suggesting increased

247 variability in response of bacterial community to pathogen infection. In fungal metacommunities, the

248 analysis revealed no significant differences between infected group and the control (PERMANOVA: R^2

249 $= 1.29$, $p > 0.05$, permutest: $F = 0.77$, $p > 0.05$) (Supplementary Table 3).

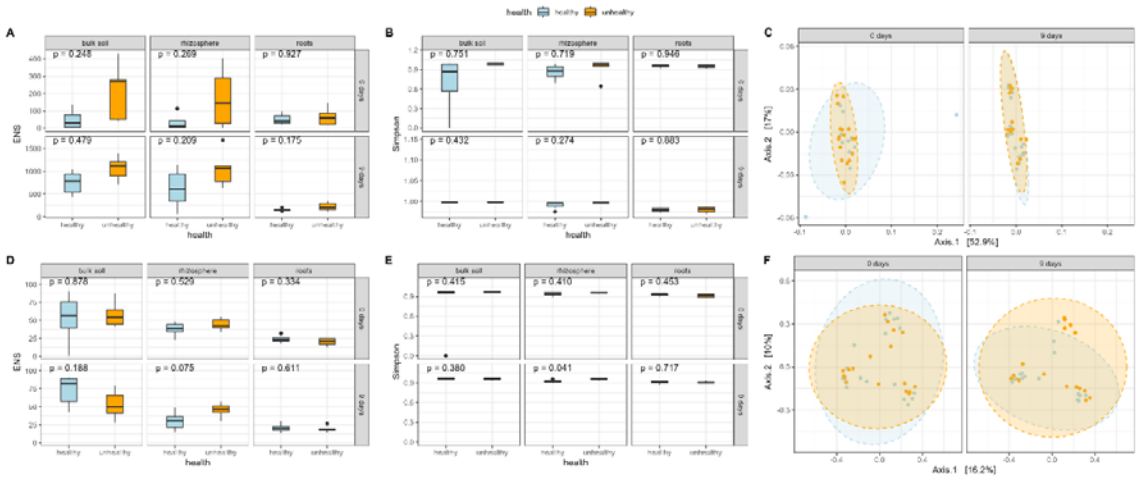

Figure 4. Comparison of alpha and beta diversity of bacterial (A, B, C) and fungal (D, E, F) communities of strawberry niches immediately after *P. lythri* inoculation (0 days) and after 9 days of (9 days). LMER model was used for comparison of non-independent samples in alpha diversity. Light blue color represents samples without pathogen inoculation, and orange - with inoculation.

To elucidate the influence of *P. lythri* on microbial migration between the niches, we used samples from sampling at 0 days as a source, and samples from sampling at 9 days as sinks. In bulk soil, only bacterial community revealed significantly higher share of microorganisms in bulk soil and a lower portion from unknown source in infected samples (Figure 5A). Furthermore, we observed migration of bacteria from bulk soil to rhizosphere for both bacteria and fungi in infected communities, but also from rhizosphere to rhizosphere for bacteria in infected communities. Finally, analysis revealed increased migration from rhizosphere to roots in infected samples in bacterial community.

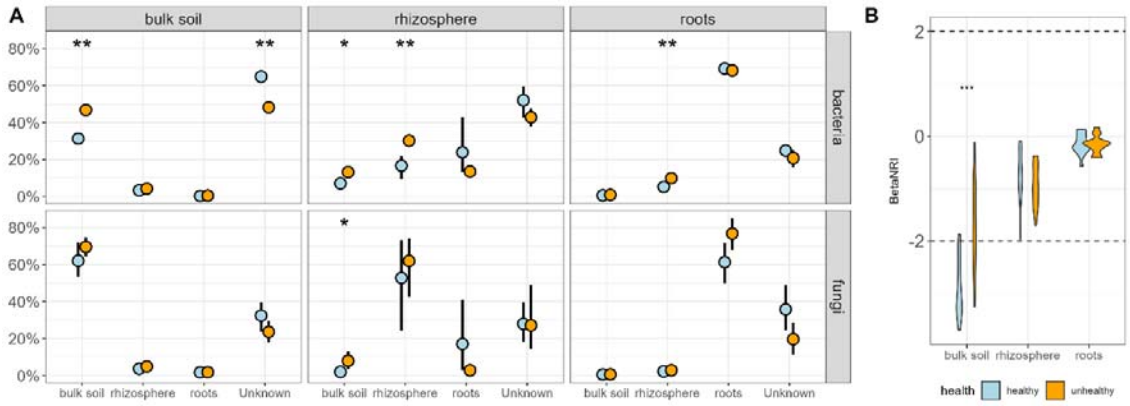

Figure 5. Source tracking analysis (A) of bacterial and fungal microbiomes between sampling one (source) and two (sink). Comparison between healthy (light blue, left) and contaminated (light orange, right) samples. Values are shown as mean

standard error from bootstrap. (B) BetaNRI index analysis of bacterial community in second sampling. Significant differences on both panels between healthy and contaminated samples are shown with asterisk.

We also evaluated the mechanisms involved in bacterial community assembly by calculating the betaNRI index for bulk soil, rhizosphere, and root samples collected during the second sampling period (Figure 5B). The results revealed a dominance of stochastic processes in both healthy and infected rhizosphere and root samples of strawberry (betaNRI values between -2 and 2). Furthermore, we observed differences in community assembly processes between healthy and infected bulk soil, with a shift from deterministic processes (characterized by lower turnover) in healthy bulk soil to a dominance of stochastic processes in infected soil.

Finally, to evaluate the influence of *P. lythri* on the structure of fungal community, we compared the network structure in the rhizosphere niche between control and infected samples during the second sampling (Figure 6, Supplementary Figure 3, Supplementary Table 5). Both networks showed similar characteristics in terms of the number of components (1), clustering coefficient (0.995, 0.999), modularity (-0.007, -0.008), edge density (0.994, 0.999) and natural connectivity (0.375, 0.310), average dissimilarity and average path length (0.6, 0.6). On the other hand, the control rhizosphere exhibited a higher percentage of positive edges (52.308% vs. 43.344%) but lower vertex and edge connectivity (58, 71).

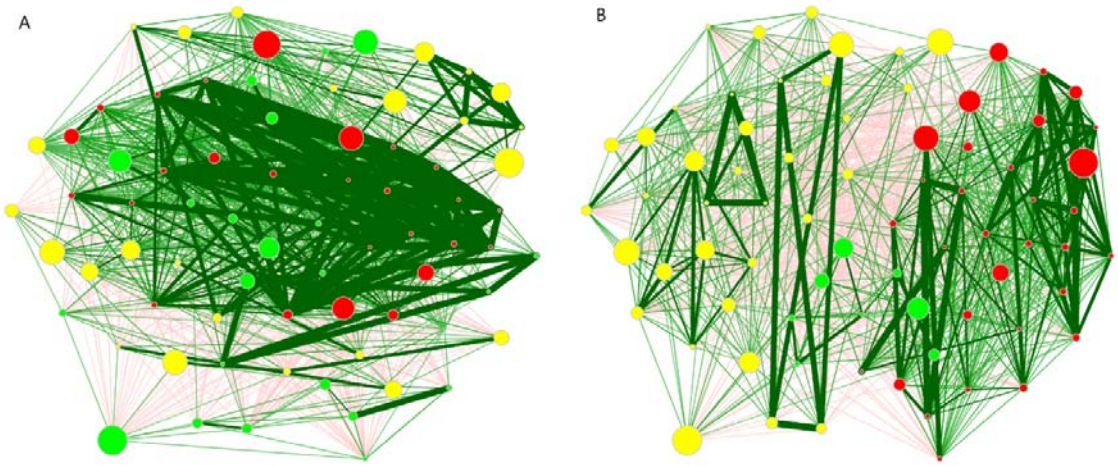

Figure 6. Fungal network analysis in A) control and B) pathogen-inoculated rhizosphere samples of strawberry. Each node represents individual fungal ASV, and node size is proportional to number of reads. Node colours represent the same

clusters. Green lines represent positive interactions and red- negative. The position of the same nodes is the same in both networks.

Notably, changes were observed in centrality of networks (Jaccard Index). Degree, betweenness and hub taxa measures showed no overlap in most connected, keystone and key hub taxa, significant shift was observed in closeness of most central nodes (Table 1).

Table 1. Centrality changes between networks of rhizosphere samples in control and *P.* contaminated samples. Asterisk shows statistically significant change.

	Degree	Betweenness	Closeness	Eigenvector	Hub taxa
Jaccard Index	0	0	0.071	0.209	0
p-value (P≤Jacc)	1	0.296	0.027*	0.055	1

Importantly, *Pilidium* was identified as a connector taxa in the control rhizosphere (betweenness = 1), loosing this status in pathogen-inoculated (betweenness = 0) samples (Supplementary Table 5).

Discussion

Here, we investigate the underexplored role of emerging thermotolerant fungal pathogen in shaping plant microbiomes using newly isolated strains of *Pilidium lythri*. We assessed its thermal tolerance by screening metabolic response to 120 different chemical substances and explored its impact on the structure, assembly processes and association networks of bacterial and fungal metacommunities across strawberry soil and plant niches (bulk soil, rhizosphere, roots).

In vitro evaluation of the impact of various chemical substances on the growth and development of the tested phytopathogen at two temperatures (24 and 30 °C) using BIOLOG microarrays raised serious concerns, as *P. lythri* demonstrated overall higher metabolic activity at higher temperatures. This aligns with the growing evidence of global warming contributing to the spread of fungal phytopathogens to new areas (Ward *et al.*, 2007; Bebber *et al.*, 2013; Chaloner *et al.*, 2021). Among the 120 chemical substances tested, top five presented inhibition mechanism on pathogens

307 metabolic activity, likely by disruption of electron chain, destabilization of cell membranes, and
308 inhibition of DNA/RNA synthesis (Waldorf and Polak, 1983; Mamouei *et al.*, 2018; Ansari *et al.*, 2024;
309 Yang *et al.*, 2025). Unfortunately, although significant, the effect of the inhibition was modest. These
310 results underline high resilience of the pathogen that points to its high environmental tolerance and
311 potential to spread.
312 While the dissemination of fungal pathogens is widely reported (Bebber *et al.*, 2013), still little is
313 known about the effect of such invasive microorganisms on the microbial structure of the plant
314 holobiont. A number of studies have reported significant differences in the α-diversity of microbiome
315 structure between healthy and infected soil and plant niches (Lefcheck *et al.*, 2015; Delgado-
316 Baquerizo *et al.*, 2016; Bakker *et al.*, 2018). In the present study, we compared alpha and beta
317 diversity of bacterial and fungal metacommunities in healthy and *P. lythri*-infected bulk soil,
318 rhizosphere, and roots at two time points: directly after pathogen inoculation and 9 days post-
319 inoculation. For the bacteria, alpha diversity did not differ between inoculated and control samples,
320 but we observed increased community dispersion, that points to possible destabilization of bacterial
321 assemblages under biotic stress. To test this, we analyzed the mechanisms involved in bacterial
322 microbiome assembly. The results indicated that composition of bacterial communities in healthy
323 and diseased rhizosphere and roots samples was shaped by stochastic processes (i.e. random
324 colonization, dispersal, and ecological drift). Interestingly, we observed a shift from deterministic
325 processes in healthy bulk soil, to stochastic processes in *P. lythri*-infected samples, indicating a
326 disruption in microbial turnover. Infected soil showed random processes that could have been
327 triggered by disturbances in microbial community caused by the infection, described by the Anna
328 Karenina Principle (AKP) (Arnault *et al.*, 2023). Analysis of microbial migration suggests increased
329 migration of bacteria from the soil in pathogen-inoculated samples, as well as increased migration of
330 bacteria from the rhizosphere to the roots in infected plant samples. This inconsistency between
331 migration (suggesting plant filtering) and microbial assembly (suggesting random processes) could be
332 caused by the smaller scale of deterministic processes being masked by larger-scale microbial

333 community assembly. Furthermore, these two mechanisms represent different time scales, where
334 βNRI focuses on broader, longer-term assembly processes (Arnault *et al.*, 2023). Importantly,
335 migration of microorganisms can be caused by random dispersal (stochastic processes) but may
336 appear deterministic as migration increases. Thus, these two processes are not necessarily
337 contradictory.

338 In the fungal microbiome, we observed increased migration of fungi from bulk soil to the rhizosphere
339 in the inoculated samples compared to control, highlighting the importance of this niche in fungal
340 microbiome dynamics and the role of plant in microbial recruitment under pathogen stress (Bais *et*
341 *al.*, 2006; Berendsen *et al.*, 2012). The alpha diversity results revealed an increased diversity of the
342 fungal community under pathogen influence in the strawberry rhizosphere, and we then compared
343 the microbial networks in this niche to further explore the influence of the pathogen. A number of
344 methods for construction and analysis of co-occurrence networks had been developed, and SPIEC-
345 EASI is characterized with important advantages, such as accounting for compositional type of data
346 and mitigation of non-independence of samples. Also, an implementation of glasso approach allowed
347 for the analysis in high-dimensional setting with more variables than samples (Kurtz *et al.*, 2015).
348 Thus, we implemented these methods for the analysis in current study. Comparison of healthy and
349 infected samples revealed shift in microbial fungal networks under *P. lythri* influence. The fungal
350 networks in infected rhizospheres exhibited lower percentages of positive edges compared to
351 control, and lower robustness of networks, suggesting restructuring of fungal community in response
352 to pathogen presence. These findings underline decrease in natural connectivity percentage of
353 positive edges, that suggest lowered positive interactions between fungal taxa. Infection with the
354 pathogen significantly disrupted fungal networks, by decreasing networks connectivity, which
355 indicates a shift toward increased competition and antagonism within the fungal microbiome. This
356 suggests adaptation of the fungal meta-community, making it more resistant to further infections
357 and environmental stressors (Hernandez *et al.*, 2021).

Concluding, in this study, we isolated and molecularly identified isolates of spreading fungal phytopathogen from symptomatic strawberry plants - *P. lythri*. We observed pathogen's high tolerance to various chemical substances in both, lower and higher temperature, highlighting it hight thermal plasticity and resilience. We also noted significant variability in tolerance caused by chemical substances between strains. We used *P. lythri* to evaluate ecological impacts of spreading fungal phytopathogen on microorganism metacommunities in bulk soil, rhizosphere and roots of strawberry with high-throughput marker sequencing. We revealed that *P. lythri* infection had a major effect on both the structure and dynamics of the plant associated microbiome. Its ability to shift bacterial microbial assembly mechanism from deterministic to stochastic in the bulk soil, underscores its capacity to destabilize plant-associated microbiomes. Additionally, we observed that *P. lythri* shifted the fungal microbiome dynamics in the strawberry rhizosphere towards reducing mutualistic connections, while maintaining overall network stability. This underlined adaptive reorganization of fungal community, potentially increasing resilience to secondary infections and other (a)biotic stresses.

These findings underline the critical role of emerging, thermotolerant fungal pathogens like *Pilidium lythri* in destabilizing soil microbiomes and plant-microbiome interactions. This is significantly important in the context of global warming, which accelerates spread and impact of such pathogens.

Author Contribution

Conceptualization: DS, MF, JP, Data curation: DS, JP, Formal analysis: DS, Funding acquisition: DS, Investigation: DS, JP, Methodology: DS, JP, MF, EH, Project administration: DS, Resources: MF, DS, EH, Software: DS, JP, EH, Supervision: DS, Validation: DS, Visualization: DS, Writing – original draft: DS, Writing – review & editing: DS, EH, JP, MF

Acknowledgments

This research was funded in whole by National Science Centre, Poland, contract number: 2022/45/N/NZ9/02089. For the purpose of Open Access, the author has applied a CC-BY public

copyright license to any Author Accepted Manuscript (AAM) version arising from this submission. The DS's 3-month visit at the Institute of Environmental Sciences, Leiden University, Leiden, Netherlands was financed by the Polish National Agency for Academic Exchange, contract number: BPN/BEK/2023/1/00125/U/00001.

Conflict of Interest

The authors have declared that no competing interests exist.

Data Availability Statement

Metabolic profile data and R code used for ststistical analysis were deposited at gihub (https://github.com/dsiegieda/biolog_and_pot_Pilidium) for peer review purposes. After acceptance of the manuscript for publication, this data will be published in RepOD repository (https://repod.icm.edu.pl/), under permanent doi number. ITS sequences of 4 *Pilidium lythri* strains were deposited in GenBank under accession numbers: PQ632564.1, PQ632565.1, PQ632566.1, PQ632567.1. Metataxonomic sequencing data of soil and plant niches were deposited at SRA database under accession numbers: PRJNA1213298 for 16S and PRJNA1213307 for ITS. Benefits generated: benefits from this research accrue from the sharing of our data and results on public databases, as described above.

Declaration of generative AI and AI-assisted technologies in the writing process

During the preparation of original draft of this manuscript the author used ChatGPT in order to improve language and readability. After using this tool, the author reviewed and edited the content as needed and take full responsibility for the content of the publication.

References

Aguín, O., Ferreiroa, V., González-Jartín, J.M., Alfonso, A., Botana, L.M., Mansilla, J.P., and Sainz, M.J. (2018) *Pilidium lythri* is associated with bunch rot of grapevine (Vitis vinifera). *Am J Enol Vitic* **69**: 410–416.

408 Ansari, A., Kumar, D., Gupta, P., Poluri, K.M., Rai, N., Ameen, F., and Kumar, N. (2024) Mechanistic
409 insights into antifungal potential of Alexidine dihydrochloride and hexachlorophene in Candida
410 albicans: a drug repurposing approach. *Arch Microbiol* **206**: 383.

411 Arnault, G., Mony, C., and Vandenkoornhuyse, P. (2023) Plant microbiota dysbiosis and the Anna
412 Karenina Principle. *Trends Plant Sci* **28**: 18–30.

413 Arzanlou, M., Torbati, M., and Jafary, H. (2013) Fruit rot on olive caused by *Pilidium concavum* in Iran.
414 *Australas Plant Dis Notes* **8**: 117–121.

415 Ayoubi, N., Soleimani, M.J., and Zare, R. (2016) Pilidium concavum, causing tan-brown rot on
416 strawberry in Iran. *Journal of Plant Pathology* **98**: 667–669.

417 Bais, H.P., Weir, T.L., Perry, L.G., Gilroy, S., and Vivanco, J.M. (2006) The role of root exudates in
418 rhizosphere interactions with plants and other organisms. *Annu Rev Plant Biol* **57**: 233–266.

419 Bakker, P.A.H.M., Pieterse, C.M.J., de Jonge, R., and Berendsen, R.L. (2018) The Soil-Borne Legacy.
420 *Cell* **172**: 1178–1180.

421 Baldrian, P. (2016) Forest microbiome: diversity, complexity and dynamics. *FEMS Microbiol Rev*
422 fuw040.

423 Bates, D., Mächler, M., Bolker, B., and Walker, S. (2015) Fitting Linear Mixed-Effects Models Using
424 lme4. *J Stat Softw* **67**:.

425 Bebber, D.P., Ramotowski, M.A.T., and Gurr, S.J. (2013) Crop pests and pathogens move polewards in
426 a warming world. *Nat Clim Chang* **3**: 985–988.

427 Berendsen, R.L., Pieterse, C.M.J., and Bakker, P.A.H.M. (2012) The rhizosphere microbiome and plant
428 health. *Trends Plant Sci* **17**: 478–486.

429 Berg, G. (2009) Plant–microbe interactions promoting plant growth and health: perspectives for
430 controlled use of microorganisms in agriculture. *Appl Microbiol Biotechnol* **84**: 11–18.

431 Bolyen, E., Rideout, J.R., Dillon, M.R., Bokulich, N.A., Abnet, C.C., Al-Ghalith, G.A., et al. (2019)
432 Reproducible, interactive, scalable and extensible microbiome data science using QIIME 2. *Nat*
433 *Biotechnol* **37**: 852–857.

434 Bruckart, W.L., Eskandari, F.M., Coombs, E.M., Rossman, A.Y., and Palm, M.E. (2013) First report of
435 Pilidium concavum causing leaf necrosis on Fallopia japonica in the United States. *Plant Dis* **97**:
436 146–146.

437 Caesar, A.J., Lartey, R.T., and Caesar-TonThat, T. (2012) First report of *Pilidium concavum* causing
438 root lesions of meadow hawkweed in France. *Plant Dis* **96**: 1830–1830.

439 Cameron, E.S., Schmidt, P.J., Tremblay, B.J.M., Emelko, M.B., and Müller, K.M. (2021) Enhancing
440 diversity analysis by repeatedly rarefying next generation sequencing data describing microbial
441 communities. *Sci Rep* **11**: 1–13.

442 Cao, Y., Dong, Q., Wang, D., Zhang, P., Liu, Y., and Niu, C. (2022) microbiomeMarker: an
443 R/Bioconductor package for microbiome marker identification and visualization. *Bioinformatics*
444 **38**: 4027–4029.

445 Cardin, L., Vincenot, L., and Balesdent, M.H. (2009) First report of Pilidium concavum on Bergenia
446 crassifolia in France. *Plant Dis* **93**: 548–548.

447 Chaloner, T.M., Gurr, S.J., and Bebber, D.P. (2021) Plant pathogen infection risk tracks global crop
448 yields under climate change. *Nat Clim Chang* **11**: 710–715.

449 Debode, J., Van Hemelrijck, W., Heungens, K., Maes, M., and Creemers, P. (2011) First Report of
450 Pilidium concavum Causing Tan-Brown Rot on Strawberry Fruit in Belgium. *Plant Dis* **95**: 1029–
451 1029.

452 Delgado-Baquerizo, M., Maestre, F.T., Reich, P.B., Jeffries, T.C., Gaitan, J.J., Encinar, D., et al. (2016)
453 Microbial diversity drives multifunctionality in terrestrial ecosystems. *Nat Commun* **7**: 1–8.

454 Duan, Y.B., Kang, Y.B., and Yu, Z.Z. (2010) First report of *Pilidium concavum* on *Paeonia suffruticosa* in
455 China. *Plant Dis* **94**: 271–271.

456 Fernández-Ortuño, D., Bryson, P.K., and Schnabel, G. (2014) First Report of Pilidium concavum
457 Causing Tan-brown Rot on Strawberry Nursery Stock in South Carolina. *Plant Dis* **98**: 1010–
458 1010.

459 Frąc, M., Hannula, E.S., Bełka, M., Salles, J.F., and Jedryczka, M. (2022) Soil mycobiome in sustainable
460 agriculture. *Front Microbiol* **13**: 1–9.

461 Frąc, M., Jezierska-Tys, S., and Yaguchi, T. (2015) Occurrence, detection, and molecular and
462 metabolic characterization of heat-resistant fungi in soils and plants and their risk to human
463 health. *Advances in Agronomy* **132**: 161–204.

464 Garfinkel, A.R. and Chastagner, G.A. (2019) Survey reveals a broad range of fungal pathogens and an
465 oomycete on peonies in the United States. *Plant Health Prog* **20**: 250–254.

466 Geng, W.L., Hu, P., Ma, Z., Zhao, X.Y., and Wei, Y.M. (2012) First Report of Pilidium concavum Causing
467 Tan-Brown Leaf Spot on Strawberry in China. *Plant Dis* **96**: 1377–1377.

468 Gołębniak, B. and Jarosz, A. (2004) First report of tan-brown rot (*Hainesia lythri*) on strawberry fruits
469 in Poland. *Phytopathogia Polonica* **31**: 57–60.

470 Gupta, R., Anand, G., Gaur, R., and Yadav, D. (2021) Plant–microbiome interactions for sustainable
471 agriculture: a review. *Physiology and Molecular Biology of Plants* **27**: 165–179.

472 Helfer, S. (2014) Rust fungi and global change. *New Phytologist* **201**: 770–780.

473 Hernandez, D.J., David, A.S., Menges, E.S., Searcy, C.A., and Afkhami, M.E. (2021) Environmental
474 stress destabilizes microbial networks. *ISME Journal* **15**: 1722–1734.

475 Jost, L. (2006) Entropy and diversity. *Oikos* **113**: 363–375.

476 Karimi, K., Arzanlou, M., Babai-ahari, A., and Pertot, I. (2016) Biological and molecular
477 characterisation of *Pilidium lythri*, an emerging strawberry pathogen in Iran. *Phytopathol*
478 *Mediterr* **55**: 366–379.

479 Karimi, K., Arzanlou, M., and Pertot, I. (2019) Development of novel species-specific primers for the
480 specific identification of *Colletotrichum nymphaeae* based on conventional PCR and LAMP
481 techniques. *Eur J Plant Pathol*.

482 Klindworth, A., Pruesse, E., Schweer, T., Peplies, J., Quast, C., Horn, M., and Glöckner, F.O. (2013)
483 Evaluation of general 16S ribosomal RNA gene PCR primers for classical and next-generation
484 sequencing-based diversity studies. *Nucleic Acids Res* **41**: e1–e1.

485 Knights, D., Kuczynski, J., Charlson, E.S., Zaneveld, J., Mozer, M.C., Collman, R.G., et al. (2011)
486 Bayesian community-wide culture-independent microbial source tracking. *Nat Methods* **8**: 761–
487 763.

488 Kumar, S., Stecher, G., Li, M., Knyaz, C., and Tamura, K. (2018) MEGA X: Molecular Evolutionary
489 Genetics Analysis across computing platforms. *Mol Biol Evol* **35**: 1547–1549.

490 Kurtz, Z.D., Müller, C.L., Miraldi, E.R., Littman, D.R., Blaser, M.J., and Bonneau, R.A. (2015) Sparse and
491 Compositionally Robust Inference of Microbial Ecological Networks. *PLoS Comput Biol* **11**:.

492 Lefcheck, J.S., Byrnes, J.E.K., Isbell, F., Gamfeldt, L., Griffin, J.N., Eisenhauer, N., et al. (2015)
493 Biodiversity enhances ecosystem multifunctionality across trophic levels and habitats. *Nat*
494 *Commun* **6**:.

495 Liu, C., Cui, Y., Li, X., and Yao, M. (2021) microeco: an R package for data mining in microbial
496 community ecology. *FEMS Microbiol Ecol* **97**:.

497 Liu, C., Yao, M., Stegen, J.C., Rui, J., Li, J., and Li, X. (2017) Long-term nitrogen addition affects the
498 phylogenetic turnover of soil microbial community responding to moisture pulse. *Sci Rep* **7**: 1–
499 11.

500 Liu, X., Ma, Z., Cadotte, M.W., Chen, F., He, J.-S., and Zhou, S. (2019) Warming affects foliar fungal
501 diseases more than precipitation in a Tibetan alpine meadow. *New Phytologist* **221**: 1574–1584.

502 Lopes, U.P., Zambolim, L., Lopes, U.N., Pereira, O.L., and Costa, H. (2010) First report of *Pilidium*
503 *concavum* causing tan-brown rot in strawberry fruits in Brazil. *Plant Pathol* **59**: 1171.

504 Lundberg, D.S., Lebeis, S.L., Paredes, S.H., Yourstone, S., Gehring, J., Malfatti, S., et al. (2012) Defining
505 the core *Arabidopsis thaliana* root microbiome. *Nature* **488**: 86–90.

506 Malarczyk, D.G., Panek, J., and Frąc, M. (2020) Triplex Real-Time PCR Approach for the Detection of
507 Crucial Fungal Berry Pathogens—*Botrytis* spp., *Colletotrichum* spp. and *Verticillium* spp. *Int J*
508 *Mol Sci* **21**: 8469.

509 Mamouei, Z., Alqarihi, A., Singh, S., Xu, S., Mansour, M.K., Ibrahim, A.S., and Uppuluri, P. (2018)
510 Alexidine Dihydrochloride Has Broad-Spectrum Activities against Diverse Fungal Pathogens.
511 *mSphere* **3**:.

512 Marco, S., Loredana, M., Riccardo, V., Raffaella, B., Walter, C., and Luca, N. (2022) Microbe-assisted
513 crop improvement: a sustainable weapon to restore holobiont functionality and resilience.
514 *Hortic Res* **9**:.

515 Marin-Felix, Y., Groenewald, J.Z., Cai, L., Chen, Q., Marincowitz, S., Barnes, I., et al. (2017) Genera of
516 phytopathogenic fungi: GOPHY 1. *Stud Mycol* **86**: 99–216.

517 Martin, M. (2011) Cutadapt removes adapter sequences from hight-throughput sequencing reads.
518 *EMBnet J* **17**: 10–12.

519 Maússe-Sitoe, S.N., Chen, S., Wingfield, M.J., and Roux, J. (2016) Diseases of eucalypts in the central
520 and northern provinces of Mozambique. *Southern Forests: a Journal of Forest Science* **78**: 169–
521 183.

522 McMurdie, P.J. and Holmes, S. (2013) Phyloseq: An R Package for Reproducible Interactive Analysis
523 and Graphics of Microbiome Census Data. *PLoS One* **8**:.

McMurdie, P.J. and Holmes, S. (2014) Waste Not, Want Not: Why Rarefying Microbiome Data Is Inadmissible. *PLoS Comput Biol* **10**: e1003531.

Michl, K., Berg, G., and Cernava, T. (2023) The microbiome of cereal plants: The current state of knowledge and the potential for future applications. *Environ Microbiome* **18**: 28.

Milicević, T., Kaliterna, J., Ivić, D., and Milović, M. (2014) Records of phytopathogenic fungal species on native plants new to Croatia. *Natura Croatica* **23**: 179–187.

Nilsson, R.H., Larsson, K.H., Taylor, A.F.S., Bengtsson-Palme, J., Jeppesen, T.S., Schigel, D., et al. (2019) The UNITE database for molecular identification of fungi: Handling dark taxa and parallel taxonomic classifications. *Nucleic Acids Res* **47**: D259–D264.

Oksanen, J., Kindt, R., Legendre, P., O'Hara, B., Stevens, H., and Oksanen, M.J. (2007) The vegan package. *Community ecology package* **10**: 719.

Palm, M.E. (1991) Taxonomy and Morphology of the Synanamorphs *Pilidium concavum* and *Hainesia lythri* (Coelomycetes). *Mycologia* **83**: 787.

Panek, J., Frąc, M., and Bilińska-Wielgus, N. (2016) Comparison of chemical sensitivity of fresh and long-stored heat resistant *Neosartorya fischeri* environmental isolates using Biolog Phenotype MicroArray system. *PLoS One* **11**: 4–8.

Peschel, S., Müller, C.L., Von Mutius, E., Boulesteix, A.L., and Depner, M. (2021) NetCoMi: Network construction and comparison for microbiome data in R. *Brief Bioinform* **22**: 1–18.

Phatak, H.C. and Payak, M.M. (1965) *Hainesia lythri* on strawberry - a new record for India. *Indian Phytopathol* **18**: 237–239.

Pruesse, E., Quast, C., Knittel, K., Fuchs, B.M., Ludwig, W., Peplies, J., and Glöckner, F.O. (2007) SILVA: A comprehensive online resource for quality checked and aligned ribosomal RNA sequence data compatible with ARB. *Nucleic Acids Res* **35**: 7188–7196.

Rivers, A.R., Weber, K.C., Gardner, T.G., Liu, S., and Armstrong, S.D. (2018) ITSxpress: Software to rapidly trim internally transcribed spacer sequences with quality scores for marker gene analysis. *F1000Res* **7**: 1418.

Sayami, M., Babaeizad, V., and Fathi, J. (2013) First report of *Pilidium concavum* as the causative agent of tan-brown rot of *Prunus domestica* fruits. *Journal of Plant Pathology* **95**: 451.

Schoch, C.L., Seifert, K.A., Huhndorf, S., Robert, V., Spouge, J.L., Levesque, C.A., et al. (2012) Nuclear ribosomal internal transcribed spacer (ITS) region as a universal DNA barcode marker for Fungi. *Proc Natl Acad Sci U S A* **109**: 6241–6246.

Siegieda, D., Panek, J., and Frąc, M. (2024) Ecological processes of bacterial microbiome assembly in healthy and dysbiotic strawberry farms. *BMC Plant Biol* **24**: 1–14.

Siegieda, D., Panek, J., and Frąc, M. (2023) Plant and soil health in organic strawberry farms – Greater importance of fungal trophic modes and networks than α -diversity of the mycobiome. *Applied Soil Ecology* **188**: 1–15.

Stegen, J.C., Lin, X., Fredrickson, J.K., Chen, X., Kennedy, D.W., Murray, C.J., et al. (2013) Quantifying community assembly processes and identifying features that impose them. *ISME Journal* **7**: 2069–2079.

563 Torbati, M., Arzanlou, M., Abed-Ashtiani, F., and Golmohammadi, H. (2019) Occurrence of fruit rot on
564 cornelian cherry caused by *Pilidium lythri* in Iran. *Crop Protection* **125**: 104884.

565 Trivedi, P., Leach, J.E., Tringe, S.G., Sa, T., and Singh, B.K. (2020) Plant–microbiome interactions: from
566 community assembly to plant health. *Nat Rev Microbiol* **18**: 607–621.

567 Vishwakarma, K., Kumar, N., Shandilya, C., Mohapatra, S., Bhayana, S., and Varma, A. (2020)
568 Revisiting Plant–Microbe Interactions and Microbial Consortia Application for Enhancing
569 Sustainable Agriculture: A Review. *Front Microbiol* **11**: 1–21.

570 Waldorf, A.R. and Polak, A. (1983) Mechanisms of action of 5-fluorocytosine. *Antimicrob Agents*
571 *Chemother* **23**: 79–85.

572 Ward, J.R., Kim, K., and Harvell, C.D. (2007) Temperature affects coral disease resistance and
573 pathogen growth. *Mar Ecol Prog Ser* **329**: 115–121.

574 White, T.J., Bruns, T., Lee, S., and Taylor, J. (1990) Amplification and direct sequencing of fungal
575 ribosomal RNA genes for phylogenetics. *PCR Protocols: A Guide to Methods and Applications*
576 315–322.

577 Wickham, H., Averick, M., Bryan, J., Chang, W., McGowan, L., François, R., et al. (2019) Welcome to
578 the Tidyverse. *J Open Source Softw* **4**: 1686.

579 Yang, Z.H., Li, G.T., and Chen, Y. (2025) Synthesis and Antifungal Activity of Aldehydes-Thiourea
580 Derivatives as Promising Antifungal Agents Against Postharvest Gray Mold Disease. *Chem*
581 *Biodivers*.

582 Zhang, M., Li, H.L., Zhao, A.L., and Zhang, J.X. (2008) First Report of *Hainesia lythri* Causing Leaf Spots
583 of *Paeonia suffruticosa* in China. *Plant Dis* **92**: 486–486.

584

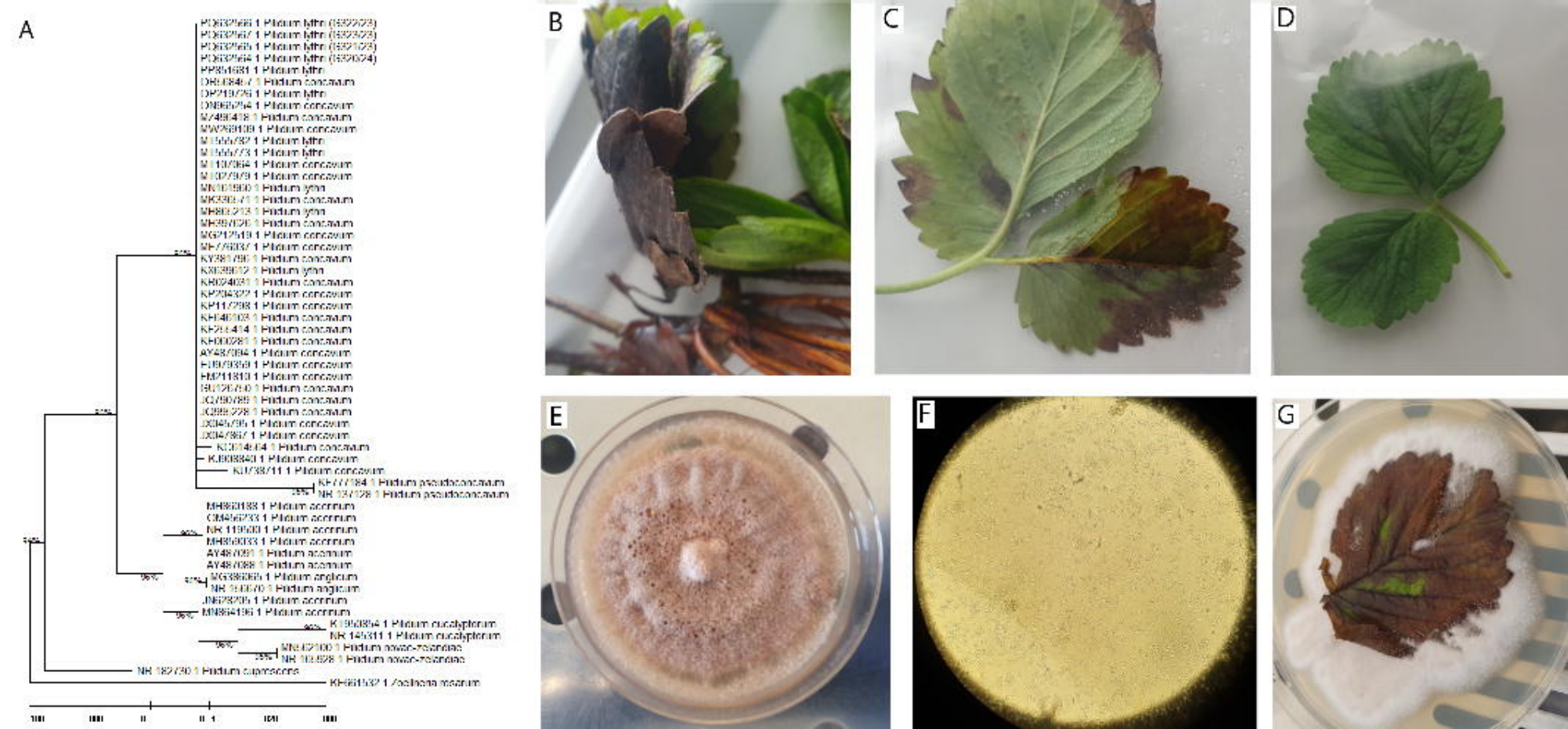
A
B
C
D
E
F
G

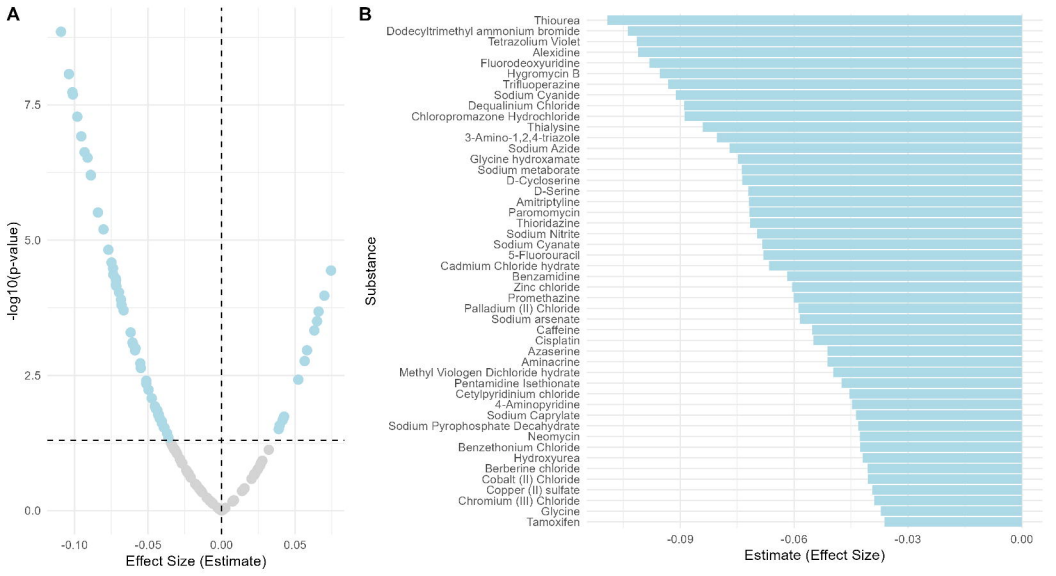
A
-log10(p-value)
7.5
5.0
2.5
0.0
-0.10
-0.05
0.00
0.05
Effect Size (Estimate)
B
Substance
Thiourea
Dodecyltrimethyl ammonium bromide
Tetrazolium Violet
Alexidine
Fluorodeoxyuridine
Hygromycin B
Trifluoperazine
Sodium Cyanide
Dequalinium Chloride
Chloropromazone Hydrochloride
Thialysine
3-Amino-1,2,4-triazole
Sodium Azide
Glycine hydroxamate
Sodium metaborate
D-Cycloserine
D-Serine
Amitriptyline
Paromomycin
Thioridazine
Sodium Nitrite
Sodium Cyanate
5-Fluorouracil
Cadmium Chloride hydrate
Benzamidine
Zinc chloride
Promethazine
Palladium (II) Chloride
Sodium arsenate
Caffeine
Cisplatin
Azaserine
Aminacrine
Methyl Viologen Dichloride hydrate
Pentamidine Isethionate
Cetylpyridinium chloride
4-Aminopyridine
Sodium Caprylate
Sodium Pyrophosphate Decahydrate
Neomycin
Benzethonium Chloride
Hydroxyurea
Berberine chloride
Cobalt (II) Chloride
Copper (II) sulfate
Chromium (III) Chloride
Glycine
Tamoxifen
-0.09
-0.06
-0.03
0.00
Estimate (Effect Size)

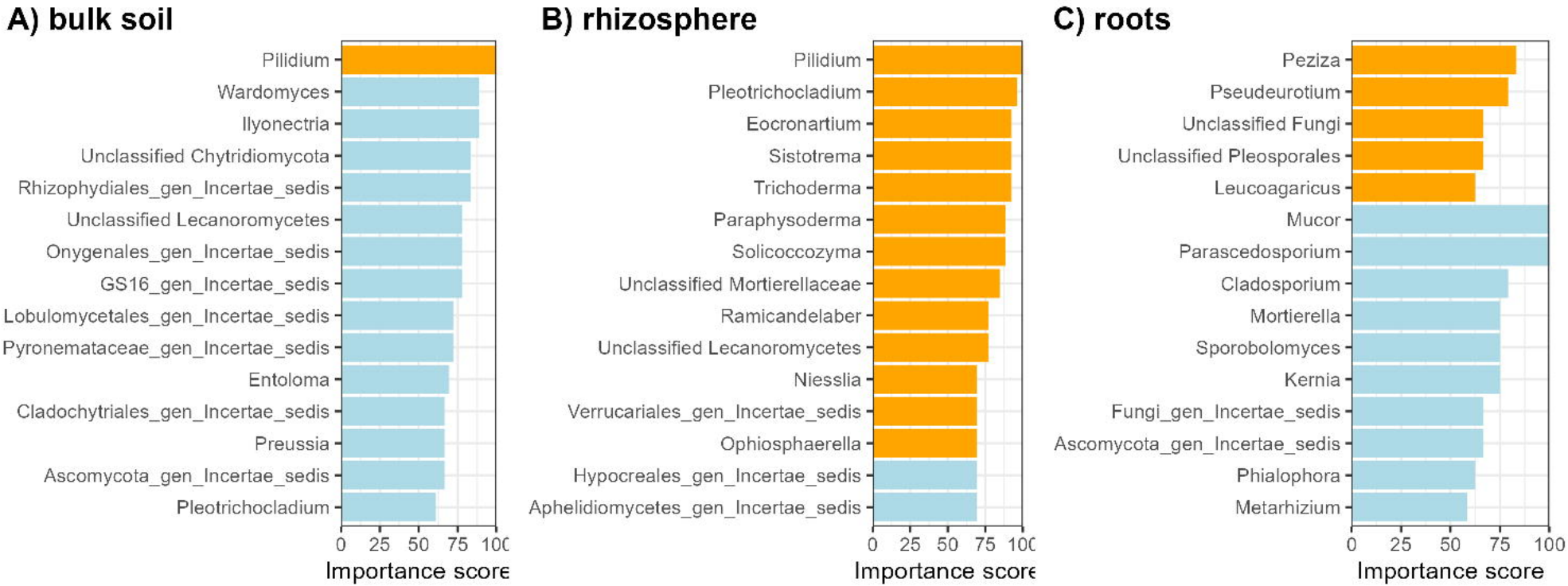
A) bulk soil
Pilidium
Wardomyces
Ilyonectria
Unclassified Chytridiomycota
Rhizophydiales_gen_Incertae_sedis
Unclassified Lecanoromycetes
Onygenales_gen_Incertae_sedis
GS16_gen_Incertae_sedis
Lobulomycetales_gen_Incertae_sedis
Pyronemataceae_gen_Incertae_sedis
Entoloma
Cladochytriales_gen_Incertae_sedis
Preussia
Ascomycota_gen_Incertae_sedis
Pleotrichocladium
0 25 50 75 100
Importance score
B) rhizosphere
Pilidium
Pleotrichocladium
Eocronartium
Sistotrema
Trichoderma
Paraphysoderma
Solicoccozyma
Unclassified Mortierellaceae
Ramicandelaber
Unclassified Lecanoromycetes
Niesslia
Verrucariales_gen_Incertae_sedis
Ophiosphaerella
Hypocreales_gen_Incertae_sedis
Aphelidiomycetes_gen_Incertae_sedis
0 25 50 75 100
Importance score
C) roots
Peziza
Pseudeurotium
Unclassified Fungi
Unclassified Pleosporales
Leucoagaricus
Mucor
Parascedosporium
Cladosporium
Mortierella
Sporobolomyces
Kernia
Fungi_gen_Incertae_sedis
Ascomycota_gen_Incertae_sedis
Phialophora
Metarhizium
0 25 50 75 100
Importance score

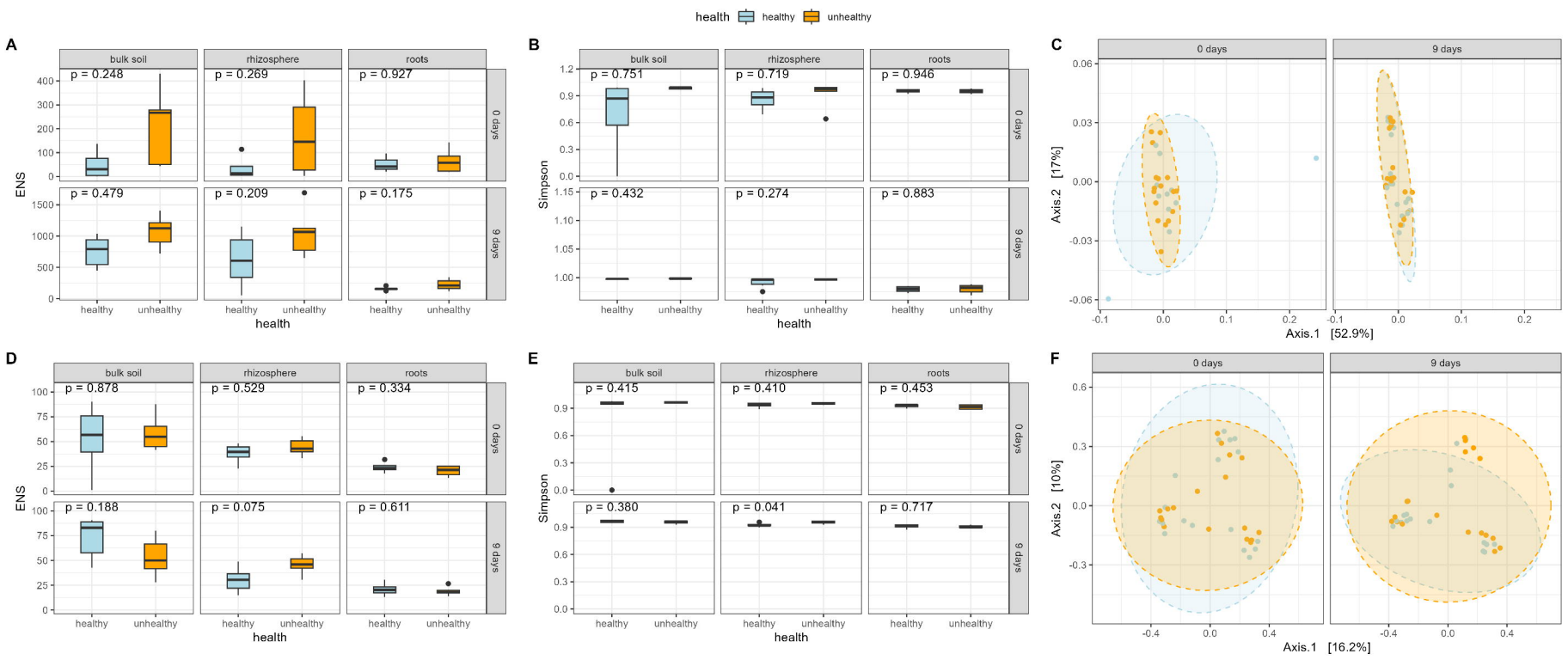
health healthy unhealthy
A
bulk soil
rhizosphere
roots
p = 0.248
p = 0.269
p = 0.927
p = 0.479
p = 0.209
p = 0.175
0 days
9 days
ENS
healthy
unhealthy
health
B
p = 0.751
p = 0.719
p = 0.946
p = 0.432
p = 0.274
p = 0.883
Simpson
C
0 days
9 days
Axis.2 [17%]
Axis.1 [52.9%]
D
p = 0.878
p = 0.529
p = 0.334
p = 0.188
p = 0.075
p = 0.611
E
p = 0.415
p = 0.410
p = 0.453
p = 0.380
p = 0.041
p = 0.717
F
Axis.2 [10%]
Axis.1 [16.2%]

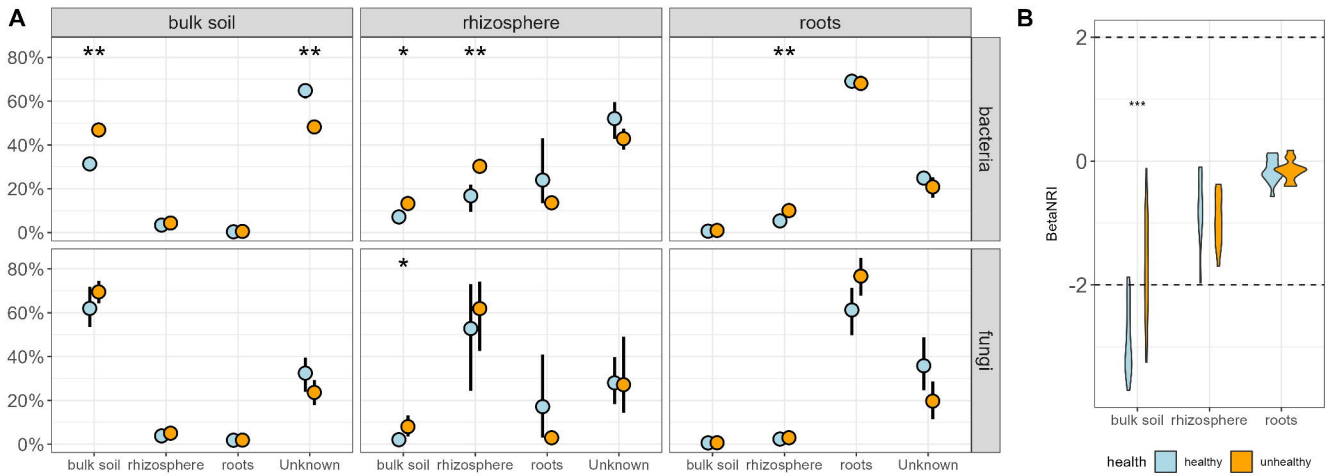
A
bulk soil
rhizosphere
roots
bacteria
fungi
80%
60%
40%
20%
0%
**
*
bulk soil
rhizosphere
roots
Unknown
B
2
0
-2
***
BetaNRI
health
healthy
unhealthy

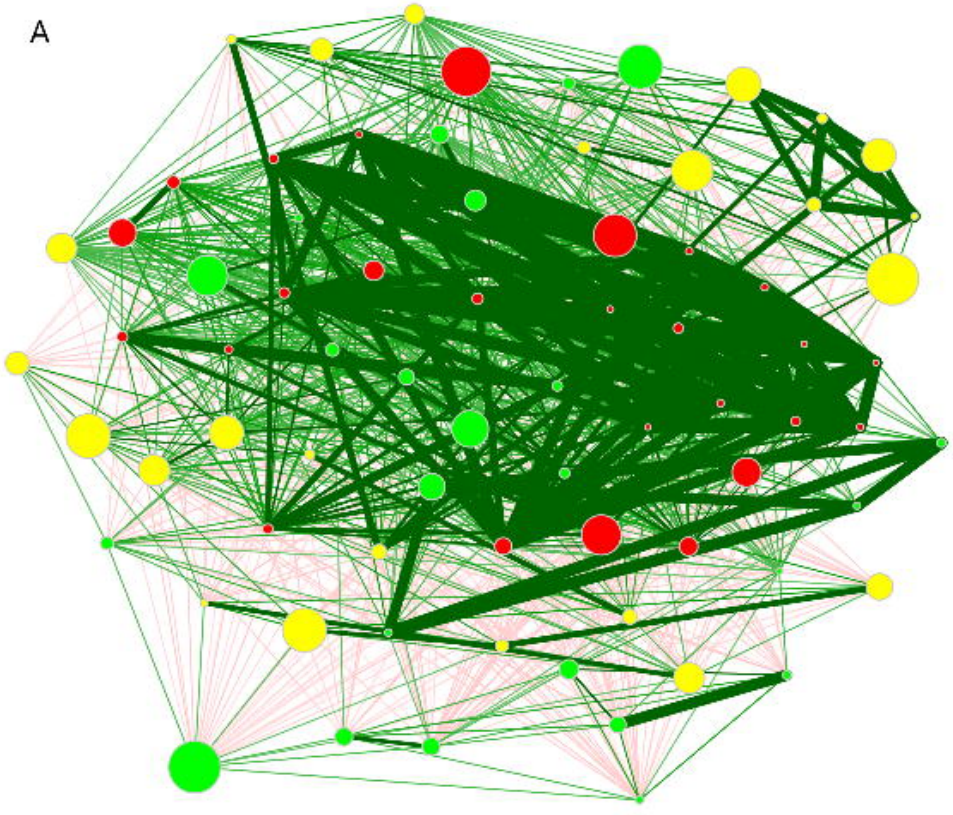
A

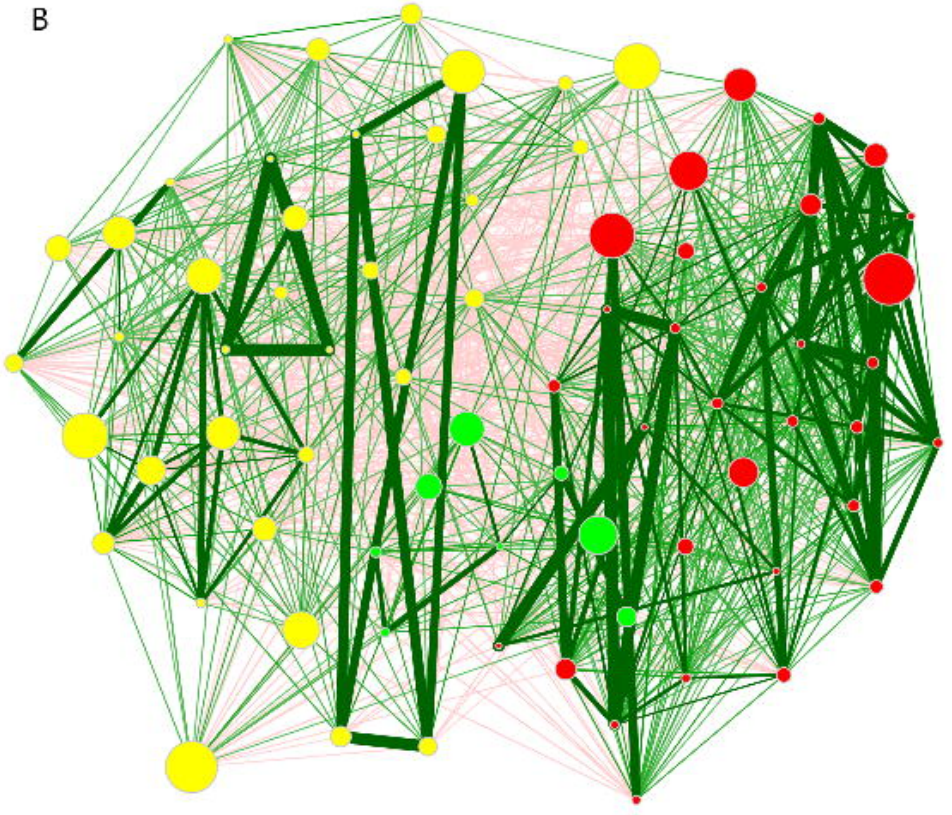
B